Article

JOURNAL OF REINFORCED PLASTICS & COMPOSITES

Journal of Reinforced Plastics and Composites
29(21) 3185–3196

DOI: 10.1177/0731684410369023
jrp.sagepub.com

SAGE

Characterization and modeling of compression behavior of syntactic foam-filled honeycombs

Rahul Jhaver and Hareesh Tippur

Abstract

Processing and compression behavior of lightweight syntactic foam-filled aluminum honeycomb composites is presented. Different foam-filled honeycomb composites are prepared by varying the volume fraction of microballoons in the syntactic epoxy foam while keeping the volume fraction of the metallic network the same. Uniaxial compression tests are then carried out on syntactic foam and foam-filled honeycomb composites. The latter shows improvement in elastic modulus and plateau stress values by 26–31% and 36–39% when compared to the syntactic foam with the same volume fraction of microballoons. The maximum increase in energy absorption for syntactic foam-filled honeycomb composite is found to be approximately 48%. The compression response and stress-strain characteristics of the foam-filled honeycombs are also examined relative to a 3D variant, namely, an interpenetrating aluminum-syntactic foam composite. Elasto-plastic finite element models are developed to simulate experiments performed on syntactic foam-filled honeycomb composite. The numerical model based on stress-strain responses of the constituents of the composite is shown to successfully capture the overall behavior.

Keywords

honeycombs, foam-filling, syntactic foam, compression tests, stress-strain response, finite element modeling

Introduction

Cellular solids[1] have attracted a great deal of attention in structural applications due to low density, high energy absorption capabilities, and good mechanical as well as acoustic properties relative to fully dense materials. For example, cellular materials made of prismatic cells as in a honeycomb are used for lightweight aerospace structural components. These materials can undergo large compressive strains while keeping the peak force to a minimum when compared to that of the solid material from which it is made. By choosing an appropriate cell wall material and relative density, foams and honeycombs can be tailored to give an optimum combination of properties for a given application. Foams and honeycombs are also commonly used as core materials in sandwich construction where the low density core increases the flexural stiffness of a structure by effectively 'thickening' it. Thereby a dramatic increase in stiffness can be achieved by a little additional weight. In recent times, foam-filled columns or sandwich panels have also replaced conventional dense metal used in industrial printer rollers and in rapidly moving platforms to reduce inertia and damp out mechanical vibrations. All these exploit the special properties offered by cellular solids which are ultimately a derivative of their microstructure.

The relative density of a cellular solid is the single most important characteristic that controls the structural properties of foams and honeycombs.[1] Filling the cellular architecture with a foam is often preferable to increasing the relative density (or increasing the cell wall thickness) of the cellular solid in order to enhance the required properties. This further increases the range of applications to meet certain stringent design

Department of Mechanical Engineering, Auburn University, AL, USA.

Corresponding author:
Hareesh Tippur, Professor, Dept of Mechanical Engineering, Auburn University, AL 36849
Email: htippur@eng.auburn.edu

requirements in which honeycombs or other single-material structural foams alone cannot be used. While the compressive performance depends on the honeycomb cell morphology, the foam-fill acts as an effective reinforcement for cell walls of the honeycomb by preventing premature bending, buckling, and shear failure besides increasing the surface area for dissipating compressive forces.* The wide range of honeycomb cell sizes and relative densities ensure many possibilities for preparing such foam-filled composites. In situations where weight is a dominant concern, low-density rigid foam can be used for making foam-filled honeycombs since the mechanical performance of foam-filled honeycomb is largely correlated to the type and density of the constituents. Thermoplastics, Nomex or aluminum honeycombs are often used as core materials in sandwich constructions and can be filled with low strength and stiffness foam for low load applications. On the other hand, high strength and stiffness foam can be used for critical applications such as aircraft structures. Furthermore, such components are damage tolerant and easy to integrate into an aerospace frame. The resulting composite core provides the strength of the honeycomb along with the workability derived from foam-filling.

Although foam-filling offers high strength to weight ratio, there are limitations on the degree of concentration of the secondary phase that can be dispersed into the primary phase and the degree of connectivity between the phases. This has inspired a relatively new category of materials called Interpenetrating Phase Composite/s or IPC. The IPC are multiphase materials in which the constituent phases are interconnected three-dimensionally and topologically throughout the microstructure. That is, both matrix and reinforcement phase/s interpenetrate all over the microstructure, *in all the three spatial dimensions*. Thus, an IPC architecture where an open-cell preform filled with polymer foam could offer an alternative method of enhancing strength and stiffness of a lightweight structure.

In this context the literature review for the present research can be classified into works on foam-filled honeycombs and foam-filled 3D scaffolds/preforms. There are a few reported results available on foam-filled honeycombs. The paper by Wu et al.[4] highlights the improvements in the mechanical properties of honeycomb core by filling it with rigid polyurethane foam. This foam-filled honeycomb was used to construct sandwich panels with graphite/epoxy composite face sheets. Their low velocity impact tests showed the sandwich panel with foam-filled honeycomb core to have a higher impact resistance. Further, the impact-inflicted core crushing was found to be highly localized when compared with the unfilled honeycomb core. Vaidya et al.[5] carried out low velocity impact tests on foam-filled honeycomb core with graphite and S2-glass fabric face sheets. Low-cost resin infusion molding process was used for preparing foam-filled honeycomb core sandwich composites. Their low velocity impact tests showed the sandwich composite with S2-glass face sheet to possess higher damage tolerance relative to the composite with graphite face sheets. Low velocity and high velocity impact response of honeycomb core with fully filled polyurethane foam and partially filled foam having carbon-epoxy face sheets was also reported by Vaidya et al.[6] A vacuum assisted resin transfer molding process was used to produce sandwich panels for mechanical testing. The results showed that the ballistic limit for partially foam-filled sandwich plate increased by 74% and those with full filling had 73% increase in the ballistic limit when compared to the unfilled core samples.

A review of interpenetrating phase composites in general[7] and IPC foams in particular can be found in the work by Jhaver and Tippur.[8] In the latter, structural foams prepared by infusing uncured syntactic** epoxy foam into aluminum open-cell scaffolds were studied. This work demonstrated the benefits of synergistic mechanical constraint between the two interpenetrating foam phases resulting in a superior compression response relative to individual constituents tested separately. That is, the IPC foam had a higher stiffness, yield, and plateau stresses compared to those for the scaffold or the syntactic foam as well as the sum of the corresponding values.

In this article the feasibility of processing syntactic foam-filled aluminum honeycomb composite is demonstrated and its compression response is studied experimentally and computationally. In the following section, experimental details of material preparation are described. The mechanical characterization of syntactic foam-filled honeycombs is presented in the section 'Compression characteristics of syntactic foam-filled honeycombs'. Relevant mechanical properties of

*A similar observation regarding the benefits of foam-filling on compression failure of tubes for improving automotive crashworthiness has been made by Santosa et al.[2] and Seitzberger et al.[3] They noted a distinct improvement in stiffness, compressive yield, and plateau stresses of foam-filled tubes relative to the unfilled ones. These works also observed the plateau stress of foam-filled columns to exceed the sum of those for unfilled tubes and foam and hence a higher energy absorption. A shorter wavelength in the resulting buckles creating more plastic folds per unit length was noted.

**Syntactic foams are multifunctional lightweight structural foams with closed-cell microstructure. They are typically processed by dispersing thin-walled ceramic *hollow* microballoons into a polymer matrix material.[9–12] Their superior dielectric properties, thermal characteristics, and energy absorption capabilities coupled with excellent buoyancy have attracted the attention of the electronic, gas distribution, and marine/naval industries alike. These foams have the potential for being excellent structural materials for both aerospace and automotive industries as well.

syntactic foam-filled honeycombs and IPC foams are compared in the section 'Comparison of SFH compression characteristics with a SF-based IPC'. In the section 'Finite element modeling of syntactic foam-filled honeycombs', the details on the development of a finite element model capable of capturing the salient experimental features are presented. The outcome of this investigation is summarized in the section 'Conclusions'.

Material preparation

Syntactic foam preparation

Epoxy-based syntactic foams of different volume fractions (20%, 30%, 40%) of hollow soda-lime glass microballoons were processed. The method involved heating epoxy resin ('epo-thin' resin from Behuler Inc., USA) to 50°C for ~45 min. Predetermined amount of microballoons (3M type K-1 hollow balloons of mean diameter ~60 μm and wall thickness ~0.6 μm, bulk density 125 kg/m^3) were added to epoxy resin and the mixture was mechanically stirred to achieve uniform distribution of the filler. Subsequently, an amine based curing agent was introduced and stirring was continued. The mixture was then placed in a vacuum chamber and evacuated down to −75 kPa (gage) pressure. Once this pressure was reached the vacuum was released and the chamber was returned to atmospheric condition. This process was repeated (about 8–10 times) until no air bubbles were observed in the mixture. When the mixture showed a tendency to gel, it was transferred into a silicone rubber mold with a blind cylindrical cavity. The increased viscosity of the mixture prevented segregation of microballoons due to buoyancy. The mixture was then cured at room temperature for a period of 48 h and the cast material was rested for a week to obtain a macroscopically homogeneous and isotropic solid. The cylindrical sample was then machined to the required dimensions. The sample length and diameter were 20 mm and 26.7 mm, respectively.

Syntactic foam-filled honeycombs

Commercially available aluminum honeycomb (made of AL 5052; nominal cell size = 3.125 mm, density = 192 kg/m^3, relative density = 6%, manufactured by Hexcel corporation, USA) core was infused with syntactic foam. A silicone rubber mold was first prepared with a blind/cavity of dimensions close to the final sample dimensions. The syntactic foam (prepared as described in the previous section) was then poured into the rubber mold just before the mixture started to gel. Subsequently a pre-cut and degreased aluminum honeycomb (of dimensions close to that of the well) was slowly lowered into the cavity filled with uncured syntactic foam. This ensured good percolation of uncured syntactic foam mixture into the honeycomb cells. The resulting composite was then cured at room temperature for 48 h before removing from the mold for machining. The sample was subsequently machined to dimensions of 25.4 mm × 25.4 mm × 16 mm after resting for a week. A photograph of the resulting sample is shown in Figure 1; the honeycomb structure along with the syntactic foam-filled cells can be readily seen in the photograph. Different varieties of syntactic foam-filled composites were prepared by varying the volume fraction of microballoons in the syntactic foam from 20–40% while keeping the volume fraction of the metallic network the same.

Compression characteristics of syntactic foam-filled honeycombs

Honeycombs are commercially produced by expanding strip-glued sheets. As a result each cell has two cell walls of twice the thickness of the sheet. This results in an anisotropic mechanical response of a honeycomb. That is, the overall response differs when loaded in the L- (longitudinal) or W- (width) directions, as shown in Figure 1.

Effect of volume fraction of microballoons

The compression response of syntactic foam-filled honeycomb (SFH) composites containing 20%, 30%, and 40% volume fractions of microballoons are shown in Figure 2. In Figure 2(a) and (b) the stress-strain responses when compressed in the L- and W-directions, respectively, are shown. In Figure 2(c) the response of syntactic foams with 20%, 30%, and 40% volume fraction of microballoons is also shown for comparison.

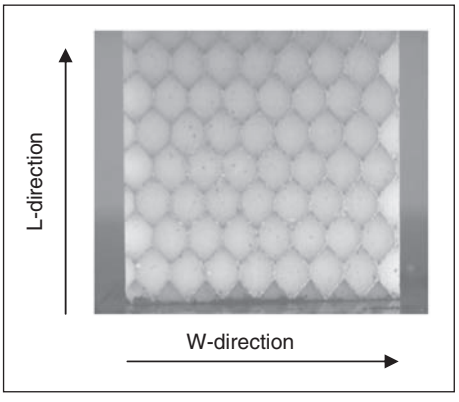

Figure 1. Syntactic foam-filled aluminum honeycomb composite.

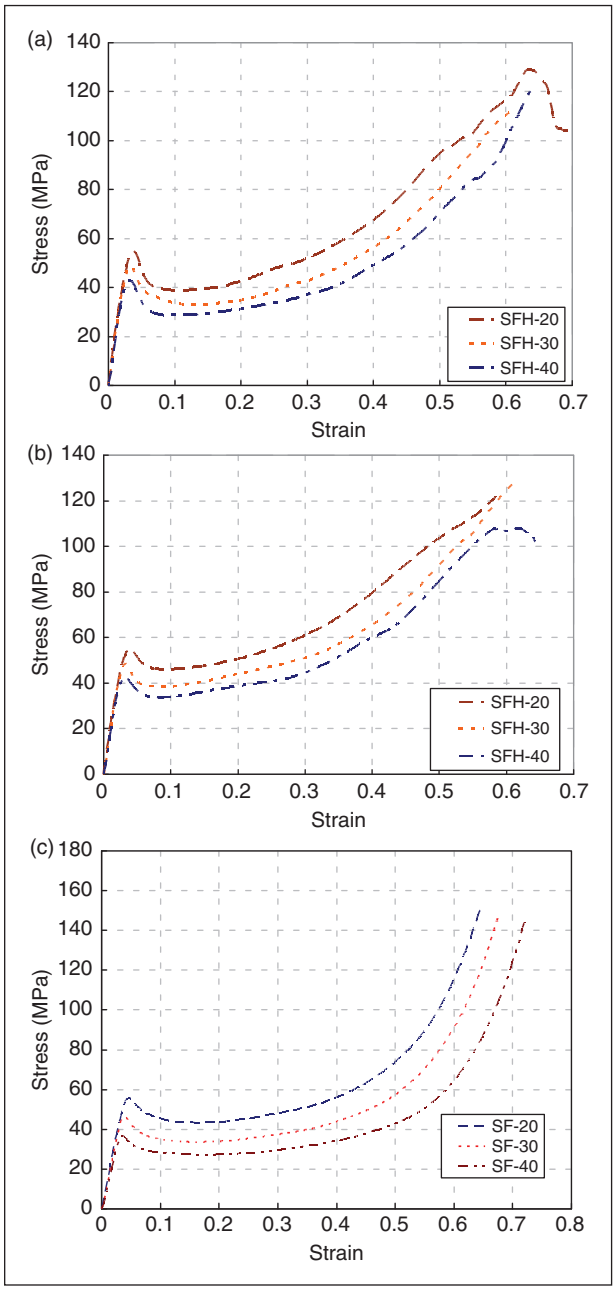

Figure 2. Compression response of syntactic foam-filled honeycomb composite. Compression along (a) L-direction, (b) W-direction, (c) syntactic foam.

From these plots, it can be seen that the general trends for syntactic foam are similar to those for structural foams in terms of the three distinct deformation regions. The linear elastic region is followed by a plateau region of nearly constant stress and a densification region of steeply rising stress. The SFH samples also show these three distinct regions. Each of these regions in this case is associated with a different deformation mechanism and was identified by photographing the foam-filled honeycomb composites during compression tests. A sequence of selected images for the case of syntactic foam-filled honeycomb containing 30% volume fraction of microballoons when compressed along the L-direction is shown in Figure 3. Upon loading, following an elastic response, the cell walls of the aluminum honeycomb network undergo bending which in turn leads to the onset of crushing of microballoons within that cell. With further increase in load, the deformation starts to localize at a small region of cells near the center and/or the corners of the specimen. In this regime, individual cells undergo deformation in a shear dominant mode. This results in deformation at a relatively constant stress level resulting in a plateau region characterized by the progressive collapse of cells. The deformation then spreads from the center (or the corners) outwards (or inwards) towards the free corners (center) of the specimen. Once this pattern evolves, crushing spreads from the collapsed zone to the neighboring cells leading to a complete failure of cells at a relatively faster rate. Upon completion of cell collapse, densification begins as seen by the region with a steeply rising stress.

From Figure 2(a) and (b) it can be seen that an increase in volume fraction of microballoons leads to a decrease in yield strength, elastic modulus, and plateau stress. The onset of densification occurs at much lower strain values when the volume fraction of microballoons in the syntactic foam is low. These trends are consistent with that observed in case of the pure syntactic foam samples in Figure 2(c). Further, these results show that the *elastic* response of SFH composite is *nearly* the same in both the L- and W-directions. (i.e., this is a relatively muted response unlike the orthotropic response of unfilled honeycombs in the L- and W-directions.[13]) The elastic modulus and plateau stress for foam-filled honeycomb composite compressed along L- and W- directions is listed in Table 1. The elastic modulus of the composite is found to decrease from 2027 ± 18 MPa for the sample with 20% volume fraction of microballoons to 1695 ± 22 MPa for the one with 40% volume fraction of microballoons. The values of plateau stress and the yield strength are also found to monotonically decrease by 22% and 26%, respectively, with increasing volume fraction of microballoons in the syntactic foam along both L- and W-directions. The graphs also show that densification strain increases with increasing volume fraction of microballoons and is not as rapid for the sample with 40% volume fraction of microballoons when compared to the ones with the lower volume fractions. With increasing density the resistance to cell wall bending and crushing of microballoons goes up resulting in higher modulus and plateau stress.

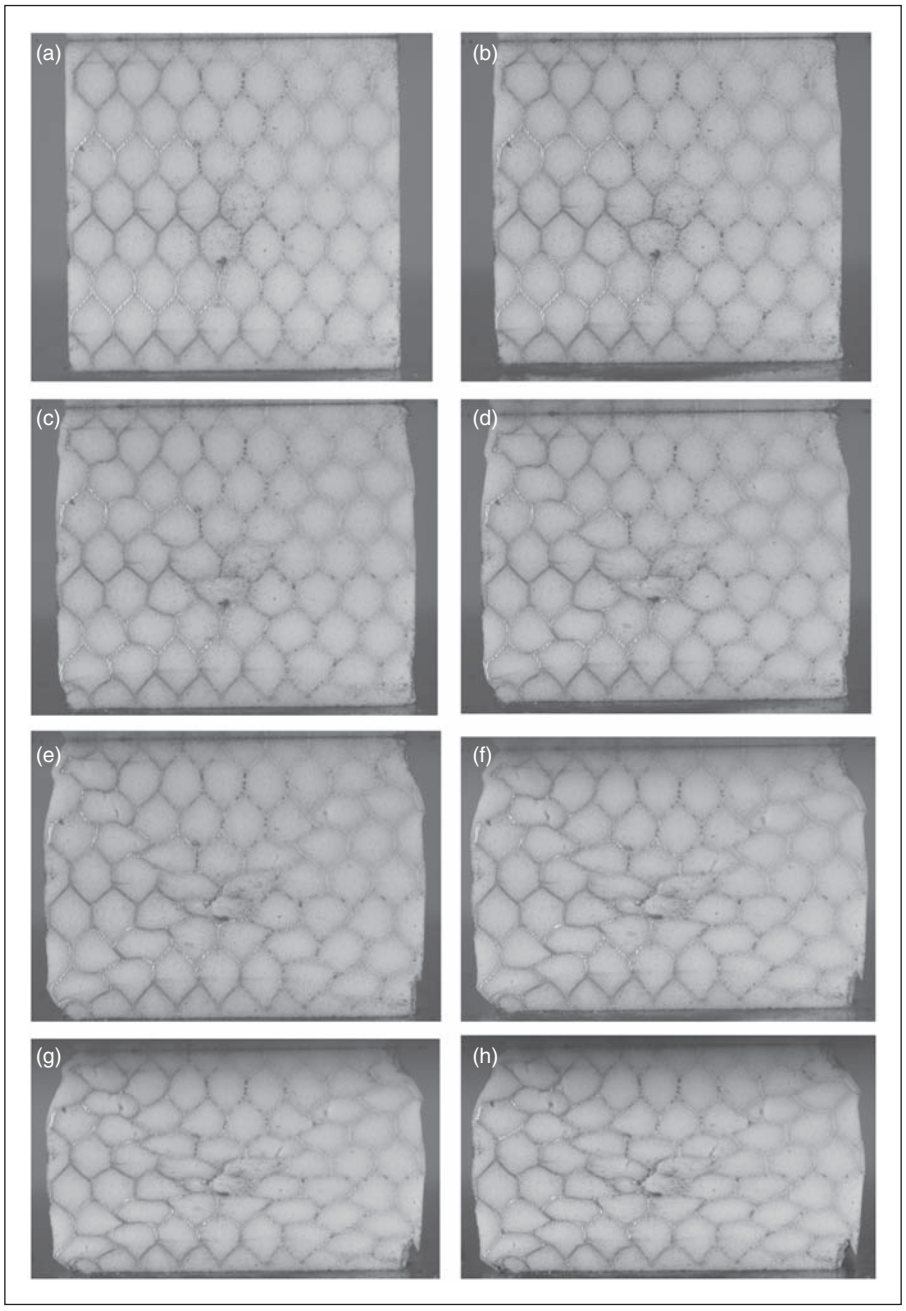

Figure 3. Photographs showing deformation sequence for a SFH-30 sample at a applied strain of (a) 0%, (b) 3.2%, (c) 5.8%, (d) 8.8%, (e) 12.6%, (f) 16.0%, (g) 24.6%, (h) 30.2%. (Compression in the L-direction).

Table 1. Properties of syntactic foam-filled honeycomb composite (20, 30, 40 designation denotes V_f of microballoons in the syntactic foam)

			L-direction	W-direction
Composite designation	Density (kg/m^3)	Elastic modulus (MPa)	Plateau stress (MPa)	Plateau stress (MPa)
SFH-20	1023 ± 8	2027 ± 18	38.58 ± 2.3	45.45 ± 2.6
SFH-30	921 ± 10	1989 ± 20	33.84 ± 1.7	38.59 ± 2.0
SFH-40	828 ± 14	1695 ± 22	28.74 ± 1.8	34.06 ± 1.6

Effect of direction of compression

The compressive response of honeycomb structures depends on whether it is compressed along the L- or the W-direction. The responses of syntactic foam and syntactic foam-filled honeycomb composites with the same volume fraction of microballoons are compared in Figure 4. In these plots, initially a linear elastic response is seen. The compressive stress decreases with increasing strain as evident from the softening response immediately following yielding. This is followed by a plateau region of nearly constant stress where progressive crushing of microballoons occurs. Further increase in load results in densification seen as a region of monotonically rising stress. The graphs show that SFH samples have the same elastic modulus and approximately the same yield stress in both the loading directions. That is, the linear elastic response is approximately isotropic and deviations between the two responses occur only at large strains in the post yielding region. For a particular volume fraction of microballoons, the foam-filled honeycomb is found to have a higher plateau stress in the W-direction when compared to the one in the L-direction. The corresponding increases are 17.8%, 14.0%, and 18.5% for 20%, 30%, and 40% volume fraction of microballoons in syntactic foam, respectively. The difference in the plateau stresses can be attributed to a non-uniform deformation and propagation of a band of diagonally deformed cells throughout the sample when compressed in the L- or W- directions.

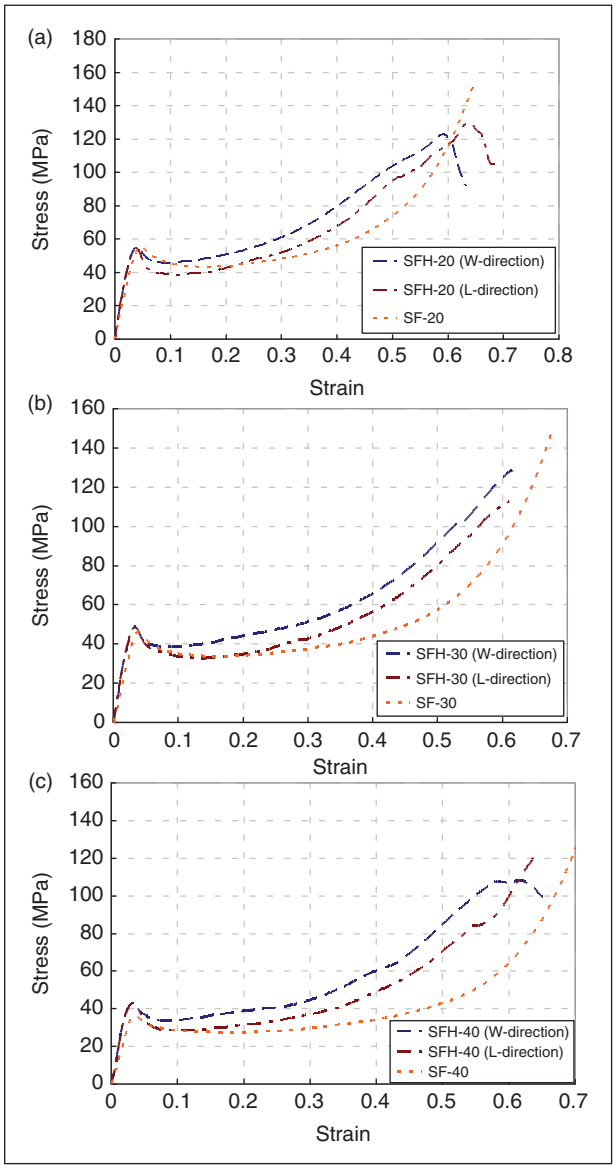

Figure 4. Comparison of stress-strain response of syntactic foam, syntactic foam-filled honeycomb for (a) 20% volume fraction, (b) 30% volume fraction, (c) 40% volume fraction of microballoons.

From Figure 4(a) it can be seen that the syntactic foam has a modestly higher yield stress when compared to the SFH specimens with 20% volume fraction of microballoons. However, this trend shifts in favor of filled honeycombs with increasing volume fraction of microballoons in SF. The yield stress of SFH is higher by ~6 MPa when compared to the pure syntactic foam (SF) with 40% volume fraction of microballoons. The increase in the volume fraction of microballoons in the foam also leads to improvements in the yield stress and plateau stress of the foam-filled honeycombs when compared to the pure syntactic foam. Hence the SFH with 40% volume fraction of microballoons shows the maximum improvement in its properties when compared to the other two volume fractions. The introduction of aluminum honeycomb network into the syntactic foam prevents the microballoons from an early collapse. This aspect is strongly manifested in the response of the syntactic foam containing 40% volume fraction of microballoons. That is, the SFH with 40% volume fraction of microballoons in syntactic foam shows significant improvements along both L- and W- directions when compared to the corresponding pure syntactic foam sample.

Energy absorption characteristics of syntactic foam-filled honeycombs

The strain energy absorbed (area under the stress-strain graphs) by the syntactic foam and the syntactic foam-filled honeycombs up to 50% strain are plotted as histograms in Figure 5. The histograms show SFH to have higher energy absorption capacity when compared

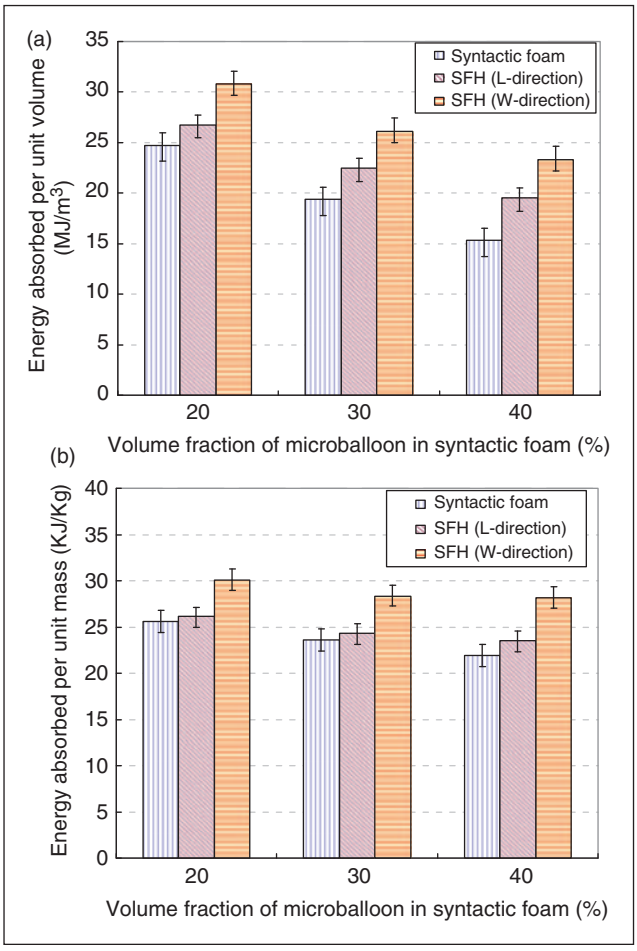

Figure 5. Comparison of energy absorption (up to 50% strain) for syntactic foams and syntactic foam-filled honeycomb (SFH) samples: (a) per unit volume (b) per unit mass.

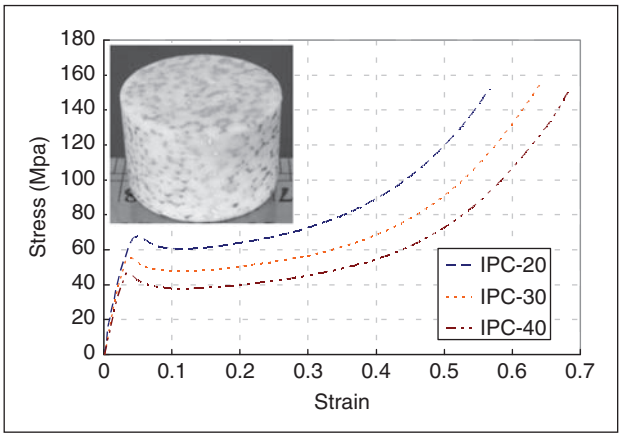

Figure 6. Stress–strain response of IPC foams specimens. Photo of the three dimensionally connected interpenetrating phase composite foam (inset). Grey network is open-cell aluminum and white regions are syntactic foam made of microballoon dispersion in epoxy.

to the corresponding syntactic foam samples made with the same volume fraction of microballoons. The foam-filled honeycomb with 20% volume fraction of microballoons, SFH-20, has the highest energy absorption with SFH-30 and SFH-40 samples showing successively lower values. From Figure 4 it can be seen that foam-filled honeycombs have higher values of plateau stress for the W-direction compression when compared to the one in the L-direction. The plots show approximately 15.1%, 16.4%, and 19.5% increase in energy absorption per unit volume of SFH-20, SFH-30, and SFH-40 honeycombs, respectively, when compressed in the W-direction compared to the corresponding values for the L-direction. The foam-filled honeycomb with 20% volume fraction of microballoons (SFH-20) has 24% higher energy absorption per unit volume when compared to the corresponding syntactic foam sample and this value increases to 34% and 48% for syntactic foam-filled honeycomb composite with 30% (SFH-30) and 40% (SFH-40) volume fraction of microballoons, respectively, when compared to the corresponding syntactic foam samples (foam-filled honeycombs are compressed along the W-direction).

The energy absorbed per unit mass is also evaluated and plotted in Figure 5(b). From the histogram it can be seen that syntactic foam-filled honeycombs compressed along the L-direction show a relatively small improvement in the energy absorption when compared to the corresponding pure syntactic foam samples. This value, however, increases for foam-filled honeycomb composites compressed along the W-direction and the percentage increase is approximately 17%, 20%, and 28% for SFH-20, SFH-30, and SFH-40 when compared to the corresponding pure SF samples. The graph also shows that the foam-filled honeycombs with 30% volume fraction of microballoons (SFH-30) and the one with 40% volume fraction of microballoons (SFH-40) have a relatively small difference in their values of energy absorption per unit mass (~0.8 KJ/Kg for the L-direction and ~0.21 KJ/kg for the W-direction). Thus if energy absorption per unit mass is a design consideration, SFH-40 appears to be as good as SFH-30 in both L- and W-directions.

Comparison of SFH compression characteristics with a SF-based IPC

Figure 6 shows stress-strain plots for different IPC foam samples from a previous work[8] by the authors.

Only limited and relevant details are provided here for comparative purposes. The IPC samples were prepared by infusing uncured syntactic foam with different volume fractions of microballoons into a preform made of aluminum network (silane coated open-cell aluminum foam manufactured by ERG Corp., CA). The relative density of the scaffold used was 6–8% (nearly same as the honeycomb used in SFH) and a pore density of 40 pores per inch. The inset in Figure 6 shows an IPC sample from that study. The compression responses of IPC samples were measured under similar loading conditions as the ones used for SFH and SF samples. The plots in Figure 6 correspond to samples made of IPC containing 20%, 30%, and 40% volume fractions of microballoons. The overall compression responses of IPC foams have similarities with the ones obtained for pure syntactic foam and syntactic foam-filled honeycomb specimens. Again, these plots show three distinct regions, typical of a structural foam behavior. Initially the response is linear elastic. The stress plateau region following the onset of nonlinearity is characterized by progressive bending of aluminum ligaments of the scaffold of the IPC foam. This in turn results in crushing of microballoons present in between the metallic ligaments.

The compression responses of IPC foam containing 20%, 30%, and 40% volume fraction of microballoons are directly compared with that of the syntactic foam-filled honeycombs in Figure 7. The IPC foams are generally found to consistently have higher yield strength and plateau stress when compared to the corresponding syntactic foam-filled honeycombs, both in the L- and W-directions. IPC-20 is found to have ~24% higher compressive strength when compared to the corresponding SFH-20 samples. This value decreases to 9.5% for composites with 40% volume fraction of microballoons. IPC-20 has the highest value for plateau stress and is found to be ~61 MPa. This value then decreases to ~39 MPa for IPC-40. Significant improvements in the compression response of IPC over SFH are clearly evident at lower volume fraction of microballoons in SF. For the 40% volume fraction of microballoons the IPC sample shows a higher plateau stress but the densification stress is found to be lower than that of the syntactic foam-filled honeycomb SFH-40 (W-direction). The crushing of microballoons and the associated mechanism of collapse is also found to be different for both the IPC and syntactic foam-filled honeycomb due to microstructural differences. The interpenetrating structure of the composite results in synergistic mechanical constraint between aluminum ligaments of the preform and pockets of infused syntactic foam. That is, aluminum ligaments are laterally supported in all three directions by the syntactic foam pockets preventing premature bending/buckling as in an unfilled preform. On the flip side, pockets of syntactic foam are reinforced by the metallic ligaments against an early crushing of microballoons.

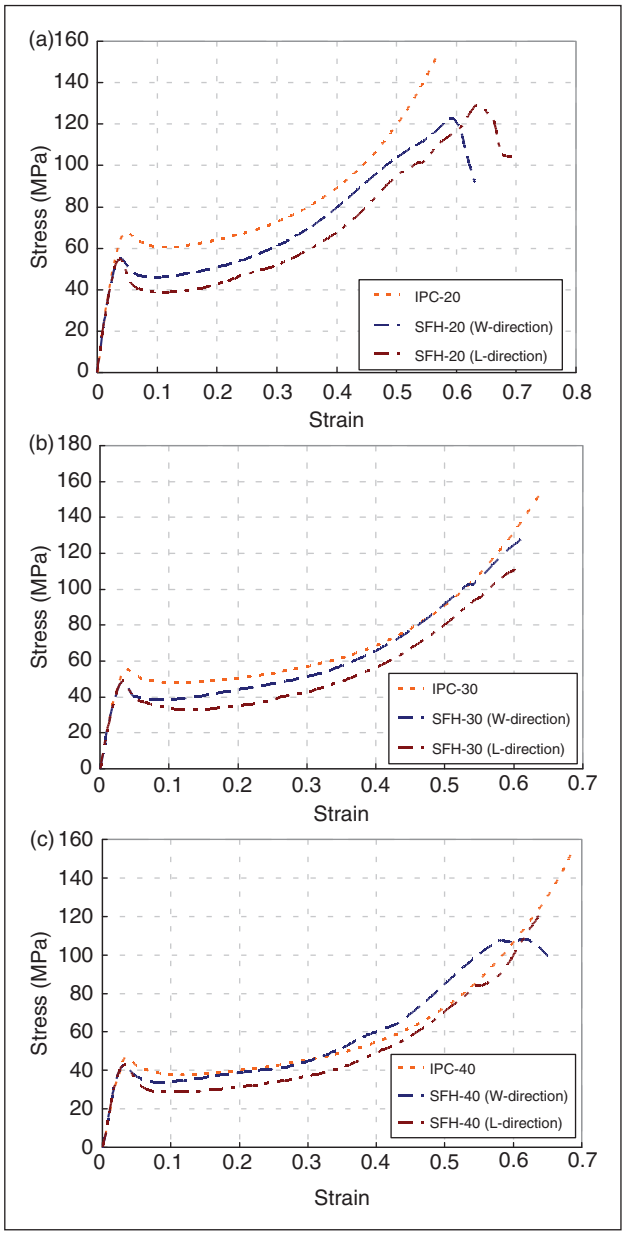

Figure 7. Comparison of stress–strain response of IPC and syntactic foam-filled honeycomb for (a) 20% volume fraction, (b) 30% volume fraction, (c) 40% volume fraction of microballoons.

Finite element modeling of syntactic foam-filled honeycombs

Full scale computational simulations were carried out to model in-plane failure characteristics of syntactic foam filled composites and also to compare those results with the ones obtained from experiments. In order to simulate the compression response of the composite, a finite element model was developed under plane strain assumptions and had the dimensions 25 mm × 25 mm × 16 mm, the same as the ones used in experiments. The wireframe structure of the composite was first modeled in MATLAB and was subsequently imported into ABAQUS structural analysis software.

Model description

The geometry for the finite element model of syntactic foam-filled honeycomb composite was generated using an array of hexagonal cells in MATLAB. First, an array of 8 × 8 hexagonal cells was generated such that each cell had a cell size of 3.25 mm (Figure 8). Next, the aluminum honeycomb structure was generated such that the area fraction of the aluminum honeycomb was 6% to be consistent with the relative density of aluminum honeycomb used in experiments.

The honeycomb sheets used in this work were manufactured using an expansion process and thus each cell had the two vertical walls of twice the sheet thickness compared to the other (inclined) sides of the cell. Accordingly, a regular honeycomb structure with double wall thickness in the vertical direction was generated to represent the aluminum honeycomb. The relative density of honeycombs was estimated by dividing the area of the cell walls by the total area of a unit cell. The material inside these cells was assumed to be filled with syntactic foam, thus resulting in syntactic foam-filled honeycomb composite. Further, the syntactic foam was assumed to be ideally bonded to the aluminum cell walls. The honeycomb sheet used for preparing SFH composite (Al 5052-H39) was same as the one studied by Papka et al.[14] These authors have developed finite element models to simulate crushing of *unfilled* honeycomb structure by assuming the stress-strain response of aluminum as a bilinear function with a post-yield modulus of $E/100$, E being the elastic modulus. Accordingly, in the current study the elastic-plastic behavior of aluminum was modeled as described in Papka et al.[14] The measured stress-strain responses for syntactic foams containing different volume fractions of microballoons were used to model the material surrounding the aluminum ligaments. A model based on associated plastic flow and von Mises yield criterion with isotropic hardening was used to model plasticity of both metallic and syntactic foam phases. The Mises yield surface was used to define isotropic yielding. In the associated plastic flow rule the direction of flow is same as the direction of the outward normal to the yield surface and in isotropic hardening the yield surface is assumed to maintain its shape, while its size increases or decreases as plastic deformation occurs. The platen of the testing machine was modeled as a rigid surface by specifying its elastic modulus to be approximately 100 times that of aluminum. MATLAB was used to construct the model which was then imported into ABAQUS finite element environment for analysis. An adaptive automatic stabilization scheme available in ABAQUS/Standard package can be used to solve unstable static problems with geometric or material nonlinearity and was also used in the current analysis.[15] A contact pair was defined between the top and bottom surfaces of the specimen that were in contact with the

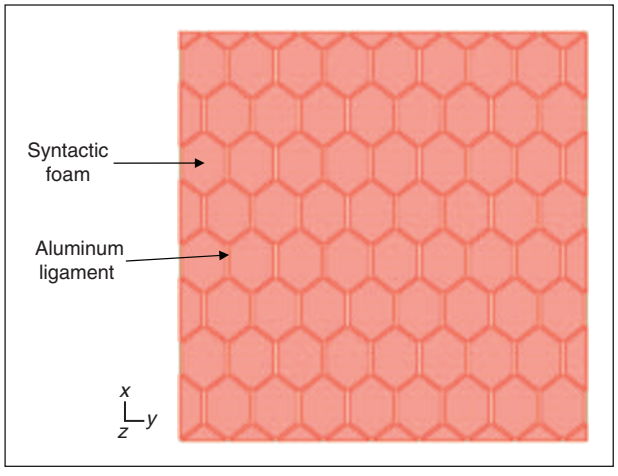

Figure 8. Geometry of honeycomb specimen used in analysis.

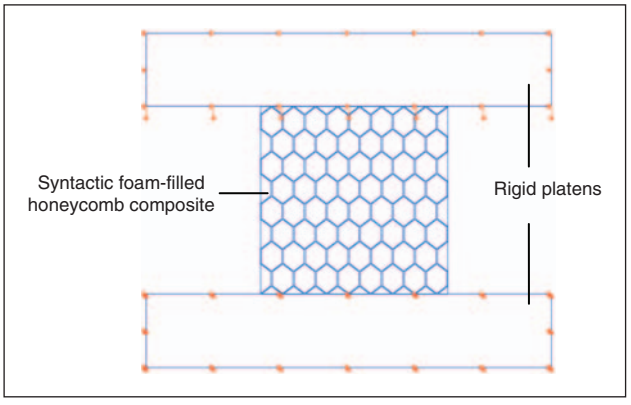

Figure 9. Loads and boundary conditions used during the analysis.

platen surface. The platen surface was chosen as the master surface and the specimen surface in contact with the platen surface was chosen as the slave surface. The normal behavior of these contact pairs was modeled using a hard contact relationship. In this relationship, any contact pressure can be transmitted between the surfaces when they are in contact and the surfaces separate if the contact pressure reduces to zero.[15] Additionally, the tangential behavior was assumed to be frictionless. Figure 9 shows the boundary conditions used in the model. To simulate experiments, the model was compressed by imposing uniform vertical displacements to the top platen as shown. The applied strain was increased from 0 to 40%.

A representative finite element mesh used is shown in Figure 10. A mesh convergence study was carried out to ensure that the refinement satisfactorily mimics experiments. The number of elements used in the finite element model for this study was varied (11140, 14354, 16760, 17983 elements) and it was found that the model with 16760 elements successfully captured the overall behavior of the composite. The model was discretized using generalized plane strain elements and a typical finite element mesh consisted of linear interpolation quadrilateral and triangular elements.

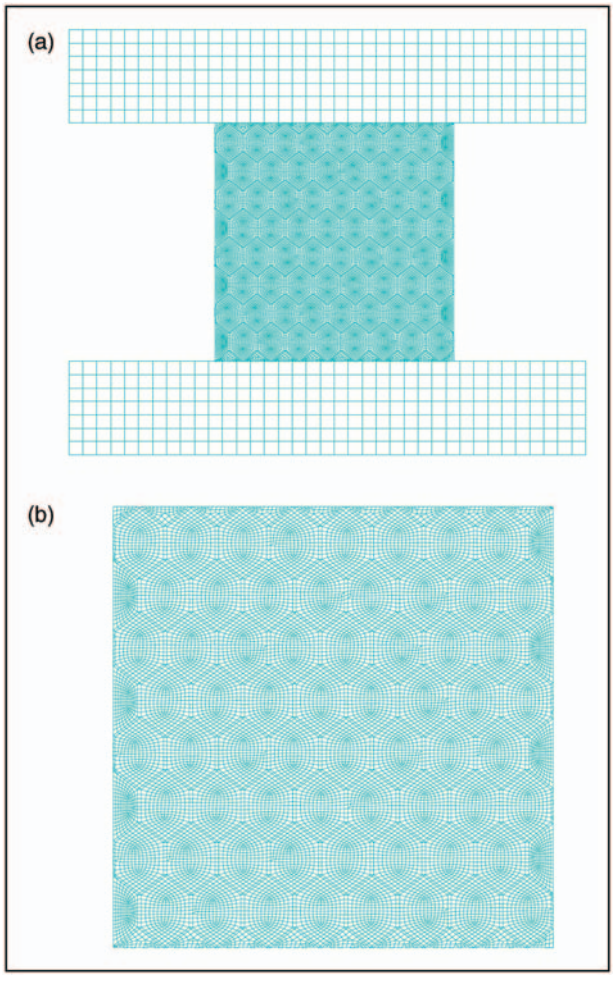

Figure 10. (a) Finite element mesh of the model (b) enlarged view showing finite element mesh of the composite.

Results

Figure 11 shows stages of deformation of a foam-filled honeycomb composite with 30% volume fraction of microballoons compressed in the L-direction. Superimposed on the deformed model are the von Mises stresses (*note that color bars correspond to different range of stresses in each figure*). A uniform vertical displacement was applied to the top platen whilst the bottom one was fixed. At relatively low applied strains (Figure 11(a)), uniform deformation of the sample can be seen. As the imposed strain increases, the deformations start to localize in a narrow band of cells in a dominant shear mode along ~45° to the loading direction, as can be seen in Figure 11(b) and (c). This leads to the formation of multiple shear bands that act as failure planes. At an applied strain of ~15% these shear bands coalesce and deformation starts spreading to the neighboring cells. The deformation process also seems to be localized with certain cells are heavily distorted while others essentially remain undeformed, similar to that observed in experiments. The deviations between the sequence of events observed during experiments and the numerical simulation can be attributed to material processing imperfections and anomalies in cell sizes of a real sample. Furthermore, the adhesive bonding of the vertical cell walls of the honeycomb are not modeled computationally. The expansion process through which the honeycombs are manufactured introduces changes in material properties and also leaves behind residual stresses as identified in Papka and Kyriakides.[16] The idealized cell geometry assumed in the finite element model does not actually exist in the honeycomb structure where the cell geometry and the cell size differ on a microscopic level. The sequence of collapse largely depends on the cell geometry and is one of the main reasons for the observed deviations. In spite of these, the global stress-strain response of the material is successfully captured by the finite element model. In Figure 12 true stress-strain response obtained computationally is compared with those obtained experimentally. The numerical model for SFH-30 seems to closely agree with the measurements over the strain window of observation. The numerical model consistently over predicts the stress by 2–4 MPa and is attributed to the idealizations used in the numerical model.

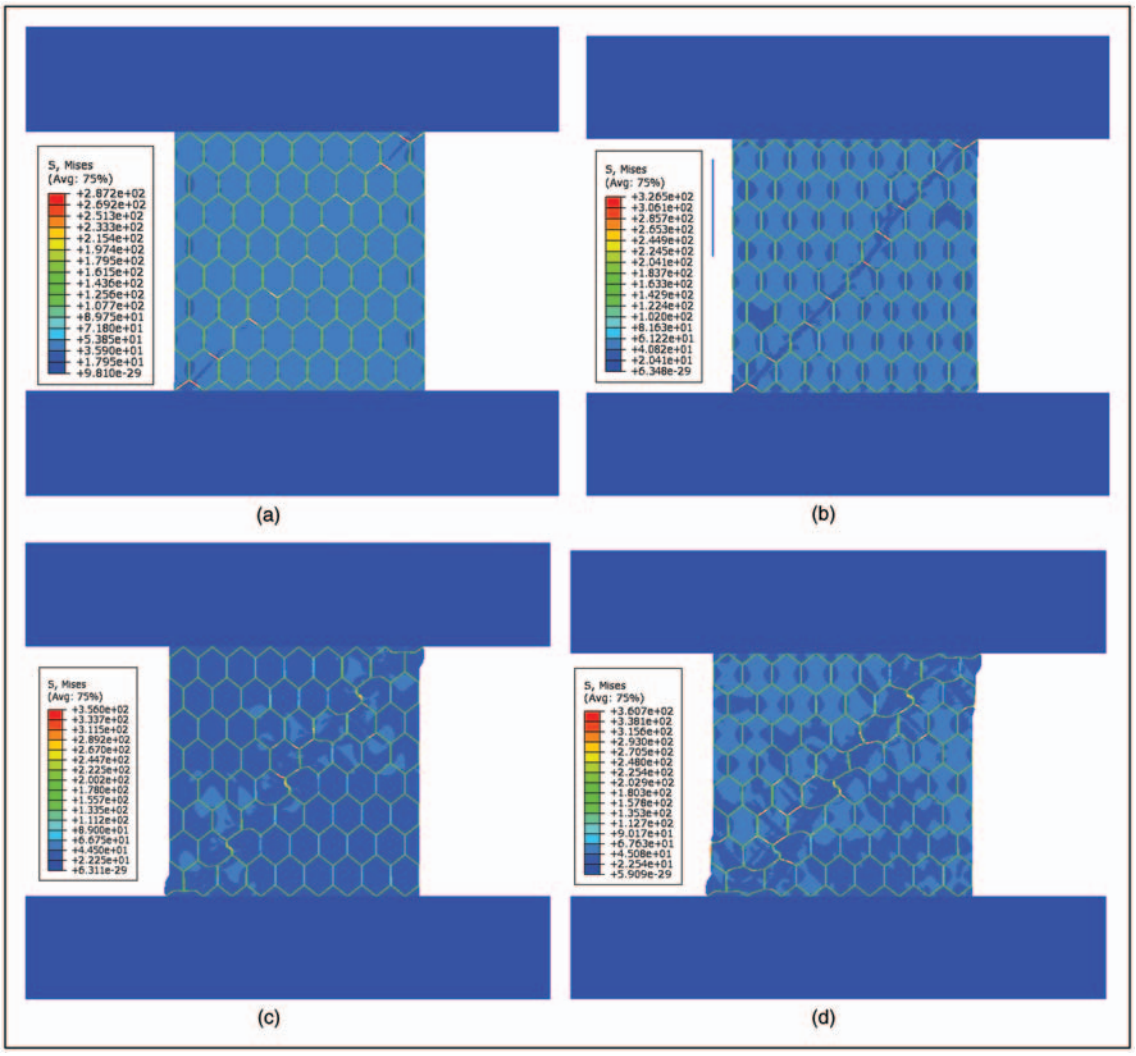

Figure 11. Sequence of deformation at applied strain of (a) 1.8%, (b) 5.4%, (c) 8.2%, (d) 14.6%. *Note that color bars correspond to different range of stresses in each figure.*

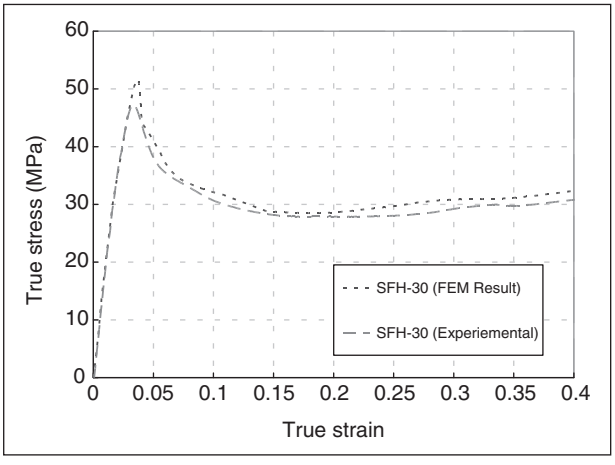

Figure 12. Comparison of numerical and experimental results (compression in L-direction) for syntactic foam-filled honeycomb composites with 30% volume fraction of microballoons.

Conclusions

The feasibility of processing lightweight syntactic foam-filled aluminum honeycomb composites is demonstrated. The foam-filled honeycombs were produced by infiltrating uncured epoxy-based syntactic foam into an aluminum honeycomb structure. Different varieties of foam-filled honeycomb composites were prepared by varying the volume fraction of hollow microballoons from 20–40% in the syntactic foam.

The syntactic foam-filled honeycombs were mechanically tested in uniaxial compression and responses were examined relative to the conventional syntactic foams with the same volume fraction of microballoons. The foam-filled honeycombs had stress-strain responses similar to the ones for conventional structural foams. An initial linear elastic response was followed by a noticeable softening caused by the onset of crushing

of microballoons leading to a plateau stress and compaction behaviors at the end. The foam-filled honeycomb composites showed 26–31% and 36–39% increase in the elastic modulus and plateau stress, respectively, along the W-direction, when compared to the conventional syntactic foam having the same volume fraction of hollow microballoons. More importantly, the foam-filled honeycomb samples had 4–8 MPa increase in the plateau stress relative to the corresponding syntactic foam samples. This also produced a rather pronounced improvement in the energy absorption in foam-filled honeycomb composites relative to the corresponding syntactic foam samples. The maximum increase in energy absorption per unit volume and energy absorption per unit mass for foam-filled honeycomb composite was found to be 48% and 28%, respectively, when compressed in the W-direction. The comparison between the stress-strain characteristics of interpenetrating aluminum-syntactic foam composite and the syntactic foam-filled honeycomb composite showed the IPC foams to consistently have higher yield strength and plateau stress due to the 3D interpenetration between phases.

Finite element models were also developed to capture the major experimental observations and the overall compressive response of syntactic foam-filled honeycomb composites. The stress-strain response of the foam-filled honeycombs was predicted by developing a full-scale (8×8 array) finite element model representing the actual experimentally studied specimens. The finite element models had the same honeycomb relative density and cell size/characteristics as the one used in experiments. The numerical model (based on measured elasto-plastic compression response of the corresponding syntactic foam and stress-strain response of aluminum) was found to successfully capture the overall behavior of foam-filled honeycomb well up to 40% imposed strain.

Acknowledgments

The authors gratefully acknowledge the support of the U.S. Army Research Office through grant W911NF-08-1-0285.

References

1. Gibson LJ and Ashby MF. *Cellular solids: structure and properties*. 2nd ed. Cambridge: Cambridge University Press, 2001.
2. Santosa S and Wierzbicki T. Crash behavior of box columns filled with aluminum honeycomb or foam. *Comput Struct* 1998; 68(4): 343–367.
3. Seitzberger M, Rammerstorfer FG, Gradinger R, Blaimschein M and Walch C. Experimental studies on the quasi-static axial crushing of steel columns filled with aluminium foam. *Int J Solids Struct* 2000; 37(30): 4125–4147.
4. Wu C, Weeks C and Sun C. Improving honeycomb-core sandwich structures for impact resistance. *J Adv Mater-Covina* 1995; 26: 41–47.
5. Vaidya U, Kamath M, Mahfuz H and Jeelani S. Low velocity impact response of resin infusion molded foam filled honeycomb sandwich composites. *J Reinf Plast Comp* 1998; 17(9): 819–849.
6. Vaidya U, Ulven C, Pillay S and Ricks H. Impact damage of partially foam-filled co-injected honeycomb core sandwich composites. *J Compos Mater* 2003; 37(7): 611–626.
7. Jhaver R. Compression response and modeling of interpenetrating phase composites and foam-filled honeycombs, MS Thesis, 2010, Auburn University, AL.
8. Jhaver R and Tippur H. Processing, compression response and finite element modeling of syntactic foam based interpenetrating phase composite (IPC). *Mat Sci Eng A-Struct* 2009; 499: 507–517.
9. Shutov FA. Syntactic polymer foams. In: *Advances in Polymer Science*. Heidelberg: Springer Berlin, 1986, vol. 73, pp. 63–123.
10. Gupta N. A functionally graded syntactic foam material for high energy absorption under compression. *Mater Lett* 2007; 61(4–5): 979–982.
11. Kirugulige MS, Kitey R and Tippur HV. Dynamic fracture behavior of model sandwich structures with functionally graded core: A feasibility study. *Compos Sci Technol* 2005; 65: 1052–1068.
12. Song B and Chen W. Dynamic compressive response and failure behavior of an epoxy syntactic foam. *J Compos Mater* 2004; 38(11): 915–936.
13. Prakash O, Bichebois P, Brechet Y, Louchet F and Embury J. A note on the deformation behaviour of two-dimensional model cellular structures. *Philos Mag A* 1996; 75(3): 739–751.
14. Papka S and Kyriakides S. Experiments and full-scale numerical simulations of in-plane crushing of a honeycomb. *Acta Mater* 1998; 46: 2765–2776.
15. ABAQUS^{TM}. *User's Manual (Version 6.7)*. ABAQUS Inc, Providence, RI.
16. Papka S and Kyriakides S. In-plane compressive response and crushing of honeycomb. *J Mech Phys Solids* 1994; 42: 1499–1532.